

MR Vessel imaging for Tumor Angiogenesis Quantification in Two Rodent Models of Hepatocellular Carcinoma

Ning Jin^{1,2}, Yang Guo², Rachel Klein², and Andrew C Larson^{2,3}

¹Siemens Healthcare, Columbus, OH, United States, ²Department of Radiology, Northwestern University, Chicago, IL, United States, ³Robert H. Lurie Comprehensive Cancer Center, Chicago, IL, United States

Introduction

Hepatocellular carcinoma (HCC) are typically hypervascular tumors. Angiogenesis, the process by which new vessels develop from pre-existing microvessels, plays an important role in HCC progression. Experimental and clinical studies indicate that patients with higher microvessel density in tumors have a poor prognosis, hence angiogenesis is regarded as an important bio-marker (1). MR vessel imaging methods, using intravascular ultrasmall superparamagnetic iron oxide (USPIO) contrast agents, has been developed to monitor tumor angiogenesis (2). Vessel size index (VSI) in micrometers, calculated based on the changes of magnetic relaxation parameters induced with USPIO agent, is independent of imaging resolution. The aim of our study was to evaluate MR vessel imaging techniques for tumor angiogenesis quantification in rat models of HCC. Two different rodent HCC models were chosen: McA-RH7777 Morris hepatoma model and N1-S1 hepatoma model.

Materials and Methods

Animal Models All studies were approved by our institutional animal care and use committee and were performed in accordance with institutional guidelines. 16 adult male Sprague Dawley rats (Charles River Laboratories, MA, USA) were used for these experiments. After anesthesia, a mini-laparotomy was performed and the left hepatic lobe exposed on a sterile compress. 5×10^6 McA-RH7777 rat hepatoma cells were visually injected into the left medial hepatic lobe in 7 rats and 5×10^6 N1-S1 rat hepatoma cells were injected using the same procedure in remaining 9 rats. 7 days were allowed for tumor growth and angiogenesis after initial implantation.

MRI All MRI studies were performed using a 3.0T Magnetom Trio Clinical scanner (Siemens Medical Solutions, Germany) with customer-built rodent receiver coil (Chenguang Medical Technologies, China). The rats were anesthetized with a high-limb injection of ketamine and xylazine. Three to five contiguous 3mm-thick axial slices were imaged to ensure the complete coverage of the entire tumor. Five datasets were acquired for each animal. First, an ADC map was calculated using the single-shot DW-SE-EPI sequence with the following b -values: 0, 50, 100, 200, 300, and 500 sec/mm². Other imaging parameters were: TR = 3 s, TE = 78 ms, FOV = 120 mm, 128×64 matrix, BW = 1500 Hz/pixel, 6 averages. DW images were acquired during free-breathing using respiratory triggering. Next, single-echo SE sequences were used to calculate T2 maps with 6 TEs (TR = 2 sec, TE = 10, 20, 30, 40, 50 and 60 ms, 4 averages). Then a MGRE sequence was used to calculate T2* map (TR = 150 ms, ETL = 12, ES = 3.06 ms). Following pre-contrast T2* mapping, 1.1 ml/kg of USPIO contrast agent (200 μ mol of iron/kg, Molday ION; BioPal, Worcester, MA) was injected via a femoral vein catheter, followed 1 ml saline. After 2 min to allow the contrast agent to circulate, the SE and MGRE scans were repeated to acquired post-contrast T2 and T2* maps.

Data Analysis Voxel-wise ADC, T2 and T2* maps were calculated by employing the non-linear Levenberg-Marquardt algorithm to fit the mono-exponential function. Blood volume fraction (BVF) and VSI were calculated according to the following equations:

$$BVF_{MRI} = (3/4\pi)(\Delta R_2^*/(\gamma\Delta\chi B_0)), VSI_{MRI} = 0.425(ADC/(\gamma\Delta\chi B_0))^{1/2} (\Delta R_2^*/\Delta R_2)^{3/2}$$

where $R_2 = 1/T_2$, $R_2^* = 1/T_2^*$, $\Delta R_2^* = R_{2,post-contrast}^* - R_{2,pre-contrast}^*$, $\Delta R_2 = R_{2,post-contrast} - R_{2,pre-contrast}$, and $\Delta\chi$ is the susceptibility difference between blood and tumor tissue in the presence of the intravascular USPIO contrast agent.

Histology CD34 staining was used as a reference standard to quantify tumor angiogenesis. Histology slices were digitized. A binary mask was created by thresholding the gray level of the blue channel. Within the whole tumor, vessel objects were detected and an area was measured (number of enclosed pixels). A mean BVF_{hist} was calculated as the total vessel area divided by tumor area. A mean vessel radius was calculated as described in prior study (3). The relationship between tumor VSI and BVF measured with MR USPIO imaging techniques and histology were assessed by calculating Spearman correlation coefficients. Mean VSI_{MRI} and BVF_{MRI} from the two tumor models were also compared using independent sample t -test.

Results

The mean ADC of McA-RH7777 and N1-S1 hepatoma models was $0.84 \pm 0.11 \times 10^{-3}$ mm²/s and $0.57 \pm 0.02 \times 10^{-3}$ mm²/s. The ADC values within the McA-RH7777 tumors were significantly higher than the ADC values within the N1-S1 tumors ($p < 0.01$). The representative BVF_{MRI} and VSI_{MRI} maps for the McA-RH7777 and N1-S1 tumors are shown in Fig 1. Fig 2 shows the representative CD34 staining for McA-RH7777 and N1-S1 tumors. Blood vessels were stained brown in the tumor region (blue background). McA-RH7777 tumors were more vascular than N1-S1 tumors. The mean BVF measure by MRI within the McA-RH7777 tumors was significantly larger compared to the value within the N1-S1 tumors ($p < 0.01$); while the VSI within the McA-RH7777 tumors was significantly lower than the values within N1-S1 tumors ($p < 0.05$). MRI measured tumor angiogenesis parameters (VSI and BV) were compared to histology angiogenesis measurements, shown in Fig 3. Statistically significant correlation was observed between BVF_{MRI} and BVF_{hist} measurements ($r = 0.758$, $p < 0.01$).

Conclusion

We observed a significant correlation between the MRI BVF and VSI measurements and the results from CD34 histology staining in two rodent HCC models. MR vessel imaging using USPIO contrast agents may potentially served as a non-invasive method to evaluate tumor angiogenesis during tumor progression in HCC.

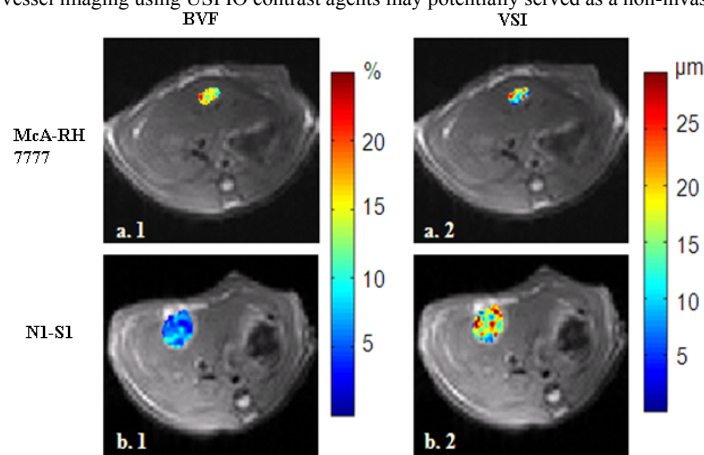


Fig 2. Representative BVF (a) and VSI (b) maps measured with USPIO MRI for McA-RH7777 (Group 1) and N1-S1 tumors (Group 2).

References: (1) Sun HC et al., J Cancer Res Clin Oncol 2004;130(6):307-319.
(2) Tropres I et al., Magn Reson Med 2001;45(3):397-408.
(3) Tropres I et al., Magn Reson Med 2004;51(3):533-541.

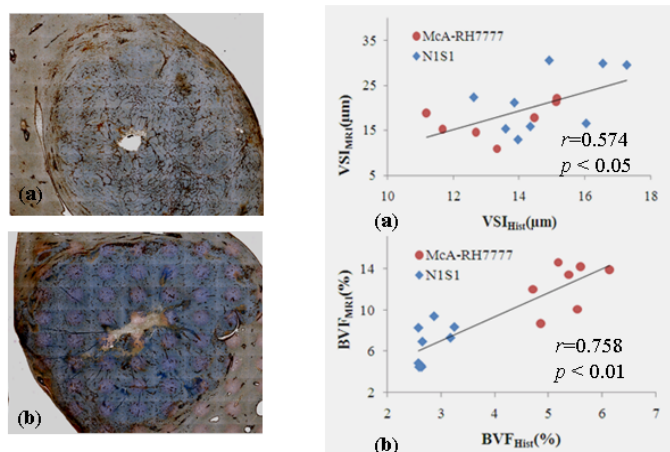


Fig 1. Representative CD34 staining for McA-RH7777 (a) and N1-S1 (b) tumors. McA-RH7777 tumors were more vascular than N1-S1 tumors.

Fig 3. Strong correlations were observed VSI_{MRI} and VSI_{hist} (a) and between BVF_{MRI} and BVF_{hist} (b)